JOURNAL OF Materials CHEMISTRY

Aerosol-assisted chemical vapour deposition (AACVD) of silver films from triphenylphosphine adducts of silver β-diketonates and β-diketoiminates, including the structure of [Ag(hfac)(PPh_3)]

Dennis A. Edwards, Robert M. Harker, Mary F. Mahon and Kieran C. Molloy*

Department of Chemistry, University of Bath, Claverton Down, Bath, UK BA2 7AY

Received 11th March 1999, Accepted 3rd June 1999

Triphenylphosphine adducts of silver β-diketonates [AgL(PPh_3)] (L = acac, dpm, tfac, hfac, fod) and β-ketoiminates (L = hfacNhex, hfacNchex) have been synthesised and evaluated as precursors for the deposition of silver films using aerosol-assisted chemical vapour deposition methodology. The 1 : 1 stoichiometry of the adducts has been established by ^{31}P and ^{109}Ag NMR and a crystal structure of [Ag(hfac)(PPh_3)]. The best films were obtained from the two β-ketoiminates, particularly L = hfacNhex. While [AgL(PPh_3)] (L = acac, dpm) gave almost no deposition, the complex with L = tfac gave a film comparable with the two β-ketoiminates while other films showed poor reflectivity (L = hfac, fod).

1. Introduction

Metal β-diketonates are known to exhibit high vapour pressures and are widely employed as precursors for CVD, for example in the deposition of metals such as Ru, Co, Rh, Ir, Pt, Cu and Au.[1–7] Thus, while AgF,[8] AgI,[9] AgO_2CCF_3,[10] $[CF_3(F)C{=}C(CF_3)]Ag$[11,12] and $[(C_5H_5)Ag(PR_3)]$[13] have all been examined for silver CVD, silver β-diketonates represent the state of the art precursors and are the largest number of precursors which have been examined (Table 1), usually as adducts [Ag(β-diketonate)L]. The main emphasis in this area has centred on the β-diketonates hfac (1,1,1,5,5,5-hexafluoro-2,4-pentanedionato) and fod (2,2-dimethyl-6,6,7,7,8,8,8-heptafluoro-3,5-octanedionato).[14–23] The adducts are generally more volatile than the uncomplexed β-diketonates and are of 1 : 1 stoichiometry save for $[Ag(hfac)(PMe_3)_2]$.[14] The nature of the Lewis base is crucial in such species, as exemplified by the olefin complexes which readily dissociate to give the relatively involatile oligomeric $[Ag(hfac)]_n$ species.[23,24] Strong metal–ligand interactions are therefore necessary to render the precursor more stable to volatilisation and to this end a number of phosphine adducts (PMe_3, PEt_3) of silver β-diketonates [β-diketonate = hfac,[15,16] fod[16,17]] have been synthesised and evaluated. These compounds were found to be low melting point solids and volatile enough to be used for conventional thermal CVD, albeit mainly at reduced pressures. It was found that hfac compounds were capable of producing metal films with 5–10% C at 310–350 °C at 10^{-2} Torr without the presence of H_2. Growth rates for [Ag(hfac)(PMe_3)] were as high as 33 nm min^{-1}, but the use of H_2 under these conditions caused premature reaction within the precursor reservoir. Adducts of Ag(fod) were found to have increased stability but required more extreme conditions to permit film growth (10^{-4} Torr, 370–380 °C). Under these conditions film quality was poor, with 16–34% C, and 4–5% O contamination. In addition, trace fluorine was found in films grown from the PMe_3 adduct, and trace phosphorus from the PEt_3 adduct. The trace phosphorus was suggested to be due to β-elimination on PEt_3 to give ethene, H_2 and phosphido groups, the latter not being so readily desorbed from the growing film.

In general, though, thermal CVD of silver films is usually accompanied by significant precursor decomposition prior to film formation[16] and alternative delivery systems are of continued interest. Recently, aerosol-assisted techniques have been used to grow silver[18] and silver alloy (Ag–Pd, Ag–Cu)[19,23] films using the precursor [Ag(hfac)(SEt_2)]. This compound was chosen to demonstrate the technique because of its insignificant volatility, which precludes its use with conventional vaporisation techniques. In this paper we assess the viability of a variety of [Ag(β-diketonate)(PPh_3)] and [Ag(β-ketoiminate)(PPh_3)] adducts which have generally been considered unsuitable for conventional CVD due to their involatility,[25] as precursors for the AACVD of silver films.

Experimental

Instrumentation

Infra-red spectra were recorded as Nujol or hexachlorobutadiene mulls between KBr plates. Measurements were made using

Table 1 CVD of silver films using silver β-diketonate adducts as precursors

Precursor	Substrate	Technique[a]	Temperature/°C	Pressure/Torr	H_2 present?	Growth rate/nm min^{-1} [b]	Ref.
Ag(hfac)(cod)	various	CVD	250	atmospheric	yes	NA	20
$Ag(hfac)(PMe_3)_n$ [c]	various	CVD	200–425	atmospheric	yes	NA	20
Ag(hfac)(PMe_3)	glass	CVD	310	0.05	no	33	15, 16
Ag(hfac)(PEt_3)	glass	CVD	250–350	0.05	no	NA	15, 16
Ag(fod)(PMe_3)	glass/Si/Cu	CVD	300	0.1	yes[d]	NA[e]	16
Ag(fod)(PEt_3)	glass/Si/Cu	CVD	230–260	0.1	yes[d]	NA	16, 17
Ag(hfac)(CNMe)	glass/Si	CVD	250	0.1	yes	NA	21
Ag(hfac)(SEt_2)	Cu coated Si	AACVD	200	atmospheric	no	40	18
Ag(hfac)(VTES)[f,g]	Si/SiO_2	CVD	160–280	0.1	no	8–16	22

[a]CVD: conventional thermal chemical vapour deposition; AACVD: aerosol-assisted CVD. [b]NA = not available. [c]$n = 1, 2$. [d]H_2 was passed through a water bubbler before entering the CVD chamber. [e]At 310 °C, 10^{-4} Torr in the absence of H_2 this precursor is reported to have a growth rate of up to 33 nm min^{-1}. [f]VTES: vinyltriethylsilane. [g]Ag(fod)(VTES) is dimeric.[22]

a Nicolet 510P Fourier transform spectrometer within the range 4000–400 cm^{-1} with a medium slit width and a peak resolution of 4.0 cm^{-1}. Carbon, hydrogen and nitrogen were determined using a Carlo-Erba Strumentazione E.A. model 1106 microanalyser operating at 500 °C. Results were calibrated against an acetanilide standard.

^{1}H and ^{13}C NMR spectra were recorded using either JEOL JNM-GX-270FT (270 MHz) or JEOL EX-400 (400 MHz) Fourier transform spectrometers using $SiMe_4$ as an internal reference. ^{19}F, ^{31}P and ^{109}Ag NMR spectra were recorded on a JEOL EX-400 (400 MHz) spectrometer; chemical shifts are relative to $CFCl_3$ [$\delta(^{19}F)$], 85% H_3PO_4 [$\delta(^{31}P)$] and 1 M $AgNO_3$ [$\delta(^{109}Ag)$]. ^{109}Ag spectra were recorded as DEPT experiments at an observational frequency of 18.45 MHz. A pulse width of 25 microseconds was used with an acquisition time of 0.744 s and a pulse delay of 10.0 s. Observable resonances were typically detected after 500–1000 scans.

Thermal analysis experiments were carried out using Dupont 951 TGA module and Dupont 910 DSC cellbase with a TA Instruments 2100 controller, at atmospheric pressure in either air-, nitrogen- or helium-purged atmospheres, from room temperature to 850 °C at a ramp rate of 25 °C min^{-1}. Samples were examined by SEM using a JEOL 6310 scanning electron microscope operating at accelerating voltages of 5, 10 or 15 kV. Coatings under investigation were not sputter coated although a path to ground was provided by means of silver dag or electrically conducting putty. Film thickness estimates using EDXS techniques were performed on a JEOL Superprobe instrument operating at an accelerating voltage of 5 kV with a beam current of 5×10^{-8} A. X-Ray counts (typically over 200 seconds) from sample films were compared against a solid silver standard. Sheet resistance was measured over a 25 mm square. Silver 'dag' busbar contacts were painted on the sample and resistance measured using a digital voltmeter. Reflection spectra at near-normal incidence were measured on a Hitachi U-3410 spectrophotometer over the range 295–2600 nm in 5 nm steps. Calibration was against rhodium standard mirrors. Reflectance data are quoted at $\lambda = 550$ nm for both the coated surface and the film–glass interface (as observed through the glass). The assessment area (corresponding to the beam size) was a rectangle of approximately 11×4 mm.

Film deposition

Details of the reactor assembly are shown in Fig. 1(top). The CVD apparatus consists of a horizontal cold wall reactor with associated gas lines and electrical heater controls. The reactor contains two separate systems, a heated bubbler assembly and an ultrasonic nebuliser line. Screening tests for this study have exclusively used the latter. The nebuliser used was an ultrasonic humidifier from Pifco Health (model no. 1077). The piezoelectric transducer, situated in the reservoir containing water, transmits ultrasound through the water and the glass of the flask into the solution to be nebulised. The distance between the piezoelectric transducer and the flask was approximately 3–4 cm. The water in the reservoir was replaced every 30 min in order to cool the transducer.

A THF solution of the precursor was poured into the three-necked round-bottomed flask and placed on the nebuliser. With the nebuliser power on the solution in the flask fountains to generate an aerosol of fine droplets (droplet size: *ca.* 0.2–5 microns). The aerosol was swept out of the flask (1.2 cm^3 min^{-1}) by a flow of nitrogen gas and transported to a horizontal cold wall CVD reactor [Fig. 1(bottom)]. The mist was first passed through a baffle to promote laminar flow, then directly into the reactor chamber (8 mm high, 40 mm wide and 300 mm long). The ceiling tile and walls of the reactor are constructed from silica. The glass substrate was positioned upon a large graphite support, which was heated

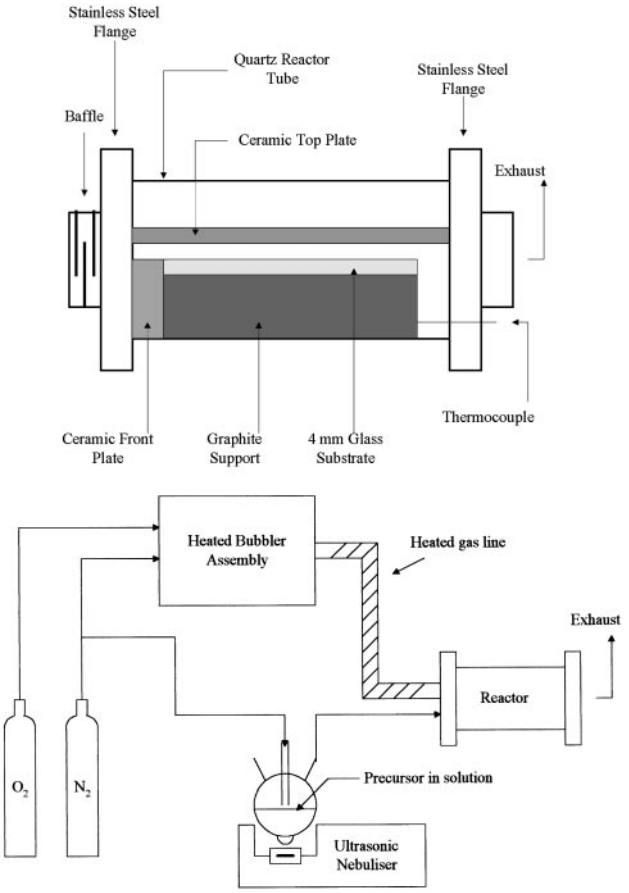

Fig. 1 Schematic diagram of the AACVD apparatus (*bottom*) and detail of the reaction chamber (*top*).

by three Watlow firewood cartridge heaters. A Watlow series 9965 controller, which monitors the temperature by means of thermocouples positioned inside the block, maintained the temperature of the graphite block. The graphite support was held inside a large silica tube (330 mm long, 100 mm diameter) suspended between stainless steel flanges upon which many of the electrical and gas line fittings are fixed. Airtight seals were provided by 'Viton' O-rings.

The films were grown at 310 °C in nitrogen held at atmospheric pressure. Typically, 0.5–0.8 g of precursor was dissolved in 40 cm^3 of THF and nebuliser flow rates were of the order of 0.8 L min^{-1}. Films were grown on glass substrates which had been cleaned immediately prior to use by washing successively with water/detergent, isopropanol and distilled water. Coating growth times were largely dependent on the volume of solvent used and carrier gas flow rates, but in all cases they were of the order of 15–30 min.

Syntheses

Synthesis of pentane-2,4-dionato(triphenylphosphine)-silver(I), [Ag(acac)(PPh_3)] (1). Silver oxide (1.50 g, 6.5 mmol) was suspended in diethyl ether (15 cm^3) and pentane-2,4-dione (1.85 ml, 1.9 g, 19 mmol) slowly added. The mixture was stirred for 5 minutes, resulting in a grey precipitate. After adding triphenylphosphine (3.39 g, 12.9 mmol), the mixture was stirred for one hour, filtered in air, and pumped dry *in vacuo.* The colourless crude product was recrystallised from diethyl ether.

Analysis: found (calculated for $C_{23}H_{22}AgO_2P$) C, 59.0 (58.9); H, 4.71 (4.73)%. IR (Nujol mull) 1200–1800 cm^{-1}: 1225, 1507, 1615. IR (hexachlorobutadiene mull) 1200–1800 cm^{-1}: 1225, 1308, 1331, 1347, 1433, 1466, 1508. ^{1}H NMR ($CDCl_3$) δ: 7.49–7.30 (m, 15H, PPh_3), 5.26

(s, COCHCO), 1.95 (s, CH_3). ^{13}C NMR ($CDCl_3$) δ: 191.0 (CO), 133.8 (d, 16.5 Hz, PPh_3), 131.5 (d, 34.2 Hz, PPh_3), 130.3 (PPh_3), 128.7 (d, 10 Hz, PPh_3), 98.5 (CO*C*HCO), 28.8 (CH_3). ^{31}P NMR ($CDCl_3$) δ: 15.1.

Synthesis of dipivaloylmethanato(triphenylphosphine)-silver(I), [Ag(dpm)(PPh_3)] (2). Silver oxide (1.5 g, 6.5 mmol) and 2,2,6,6-tetramethyl-3,5-heptanedione (2.45 g, 13.3 mmol) were suspended in diethyl ether (15 cm^3), and stirred for 5 minutes. This resulted in a cloudy grey precipitate in a black mixture. To this was added triphenylphosphine (3.4 g, 13.0 mmol) in diethyl ether (5 cm^3). The mixture was stirred for 18 hours in a closed flask in the dark to give a light grey precipitate. This was filtered in air, washed with diethyl ether, and dried *in vacuo*. Yield 6.1g, 85%.

Analysis: found (calculated for $C_{29}H_{34}AgO_2P$) C, 62.6 (62.9); H, 5.90 (6.19)%. IR (Nujol mull) 1200–1800 cm^{-1}: 1229, 1321, 1354, 1381, 1406, 1435, 1501, 1530, 1564, 1582. IR (hexachlorobutadiene mull) 1200–1800 cm^{-1}: 1229, 1354, 1385, 1406, 1435, 1449, 1480, 1501, 1530. ^{1}H NMR ($CDCl_3$) δ: 7.40–7.33 (m, 9H, PPh_3), 7.33–7.24 (m, 6H, PPh_3), 5.73 (s, COCHCO), 1.18 (s, CMe_3). ^{13}C NMR ($CDCl_3$) δ: 201.5 (CO), 134.0 (d, 16.5 Hz, PPh_3), 132.1 (d, 11.1 Hz, PPh_3), 130.2 (PPh_3), 128.8 (d, 11 Hz, PPh_3), 90.7 (CO*C*HCO), 39.4 (*C*Me_3), 27.4 (C*Me*$_3$).

Synthesis of 1,1,1-trifluoro-2,4-pentanedionato(triphenyl-phosphine)silver(I), [Ag(tfac)(PPh_3)] (3). Silver oxide (1.5 g, 6.5 mmol) was suspended in diethyl ether (5 cm^3) and 1,1,1-trifluoro-2,4-pentanedione (1.8 cm^3, 2.29 g, 14.8 mmol) slowly added resulting in the formation of a sand-coloured precipitate. To this was added triphenylphosphine (3.4 g, 13 mmol) in diethyl ether (60 cm^3), and the mixture was stirred for 20 minutes in the dark. The volume was reduced by one quarter, and the contents were filtered in air to give a sand-brown precipitate. The crude product was washed twice with diethyl ether and dried *in vacuo*. Yield 4.84 g, 71%.

Analysis: found (calculated for $C_{23}H_{19}AgF_3O_2P$) C, 52.8 (52.6); H, 3.76 (3.66)%. IR (Nujol mull) 1200–1800 cm^{-1}: 1254, 1312, 1333, 1435, 1520, 1667. IR (hexachlorobutadiene mull) 1200–1800 cm^{-1}: 1254, 1312, 1331, 1435, 1524, 1541, 1667. ^{1}H NMR ($CDCl_3$) δ: 7.50–7.40 (m, 9H, PPh_3), 7.37–7.31 (m, 6H, PPh_3), 5.50 (s, COCHCO), 1.99 (s, CH_3). ^{13}C NMR ($CDCl_3$) δ: 197.0 ($COCH_3$), 170.1 (q, 29.4 Hz, *C*OCF_3), 133.9 (d, 16.5 Hz, PPh_3), 132.0 (d, 31.3 Hz, PPh_3), 130.2 (PPh_3), 128.8 (d, 9.2 Hz, PPh_3), 119.2 (q, 289 Hz, CF_3), 92.8 (COCHCO), 30.2 (CH_3). ^{19}F NMR ($CDCl_3$) δ: −76.1 (CF_3).

Synthesis of 1,1,1,5,5,5-hexafluoro-2,4-pentanedionato-(triphenylphosphine)silver(I), [Ag(hfac)(PPh_3)] (4). Silver oxide (5.0 g, 21.6 mmol) was suspended in THF (30 cm^3) and 1,1,1,5,5,5-hexafluoro-2,4-pentanedione (6.0 cm^3, 8.8 g, 42.2 mmol) added. The mixture was stirred for five minutes, then filtered on to triphenylphosphine (11.1 g, 42.4 mmol). The resulting hazy brown mixture was stirred for five minutes, then filtered in air using a fine filter paper. The solvent was removed *in vacuo* to give a sand-coloured crystalline solid. Recrystallisation from acetone gave the title compound. Yield 21.0 g, 86%.

Analysis: found (calculated for $C_{23}H_{16}AgF_6O_2P$) C, 48.0 (47.9), H, 2.81 (2.79)%. IR (Nujol mull) 1200–1800 cm^{-1}: 1254, 1312, 1331, 1435, 1518, 1669. IR (hexachlorobutadiene mull) 1200–1800 cm^{-1}: 1254, 1312, 1331, 1435, 1480, 1522, 1541, 1669. ^{1}H NMR ($CDCl_3$) δ: 7.54–7.28 (m, 15H, PPh_3), 6.05 (s, 1H, COCHCO). ^{13}C NMR ($CDCl_3$) δ: 177.5 (q, 33 Hz, CO), 133.9 (d, 14.7 Hz, PPh_3), 131.2 (PPh_3), 130.0 (d, 40.5 Hz, PPh_3), 129.3 (d, 11.1 Hz, PPh_3), 117.7 (q, 289 Hz, CF_3), 87.9 (CO*C*HCO). ^{19}F NMR ($CDCl_3$) δ: −77.0 (CF_3).

Synthesis of tris(2,2-dimethyl-6,6,7,7,8,8,8-heptafluoro-3,5-octanedionato)pentakis(triphenylphosphine)trisilver(I), [Ag(fod)]$_3$(PPh_3)$_5$ (5). Silver oxide (1.04 g, 4.5 mmol) was suspended in diethyl ether (40 cm^3) and stirred. To this was added 2,2-dimethyl-6,6,7,7,8,8,8-heptafluoro-3,5-octanedione (2.50 g, 8.5 mmol) and a further 10 cm^3 of diethyl ether, with no immediate result. The whole mixture was stirred for one hour to give a dark brown, hazy, solution which was then filtered into a Schlenk tube containing triphenylphosphine (2.21 g, 8.4 mmol). After stirring for a further 10 min, the solution gradually cleared and was filtered using fine filter paper. The solvent was removed and the resulting solid dried *in vacuo.* Pure, colourless **5** was obtained by slow evaporation of a solution of this solid in a hexane–acetone solvent mixture at room temperature. Yield 1.4 g, 28%.

Analysis: found (calculated for $C_{120}H_{105}Ag_3F_{21}O_6P_5$) C, 57.0 (57.2); H, 3.62 (4.20)%. Mp 101 °C (by DSC/He). IR (Nujol mull) 1200–1800 cm^{-1}: 1202, 1225, 1273, 1312, 1345, 1366, 1435, 1468, 1505, 1528, 1570, 1586, 1628. IR (hexachlorobutadiene mull) 1200–1800 cm^{-1}: 1204, 1227, 1273, 1312, 1343, 1362, 1393, 1435, 1480, 1505, 1524, 1628, 1661. ^{1}H NMR ($CDCl_3$) δ: 7.50–7.31(m, 25H, PPh_3), 5.71 (s, 1H, COCHCO), 1.12 (s, 9H, CMe_3). ^{13}C NMR ($CDCl_3$) δ: 205.8 (CO), 172.0 (m, CO), 134.0 (d, 16.6 Hz, PPh_3), 131.7 (d, 33.1 Hz, PPh_3), 130.5 (PPh_3), 128.9 (d, 11 Hz, PPh_3), 119.0 (m, CF_n), 117.0 (m, CF_n), 110.8 (m, CF_n), 90.6 (CO*C*HCO), 27.9 (CMe_3). ^{19}F NMR ($CDCl_3$) δ: −81.0 (t, 9.2 Hz, CF_n), −119.7 (s, CF_n), −127.1 (s, CF_n).

Synthesis of 1,1,1,5,5,5-hexafluoro-4-(*n*-hexylimino)-2-pentanonato(triphenylphosphine)silver(I) monohydrate, [Ag(hfacNhex)(PPh_3)]·H_2O (6). 1,1,1,5,5,5-Hexafluoro-2,4-pentanedionato(triphenylphosphine)silver(I) (**4**) (5.4 g, 9.4 mmol) was suspended in benzene (150 cm^3) and hexylamine (1.2 cm^3, 0.9 g, 9.4 mmol) added. The mixture was refluxed gently in a Dean–Stark apparatus for 2½ hours with minimal decomposition. The mixture was filtered to give a deep orange solution from which a brown precipitate was obtained on concentration *in vacuo*. Yield 5.7 g, 89%.

Analysis: found (calculated for $C_{29}H_{31}AgF_6NO_2P$) C, 51.4 (51.3); H, 4.39 (4.61); N, 1.98 (2.06)%. IR (Nujol mull) 1200–1800 cm^{-1}: 1254, 1310, 1439, 1507, 1522, 1601, 1661. IR (hexachlorobutadiene mull) 1200–1800 cm^{-1}: 1254, 1310, 1435, 1482, 1532, 1563, 1611, 1671. ^{1}H NMR ($CDCl_3$) δ: 7.38–7.27 (m, PPh_3), 5.61 (s, COCHCO), 2.38 (b, 2H, CH_2), 1.43 (m, 2H, CH_2), 1.16 (m, 6H, CH_2), 0.76 (t, 6.9 Hz, 3H, CH_3). ^{13}C NMR ($CDCl_3$) δ: 175.7 (q, 31.3 Hz, CO), 133.8 (d, 16.5 Hz, PPh_3), 131.3 (d, 34.9 Hz, PPh_3), 130.6 (PPh_3), 129.0 (d, 11 Hz, PPh_3), 118.0 (q, 291 Hz, CF_3), 86.2 (CO*C*HCO), 43.5 (CH_2), 33.3 (CH_2), 31.5 (CH_2), 26.2 (CH_2), 22.5 (CH_2), 13.9 (CH_3). ^{19}F NMR ($CDCl_3$) δ: −77.2 (CF_3).

Synthesis of 1,1,1,5,5,5-hexafluoro-4-(cyclohexylimino)-2-pentanonato(triphenylphosphine)silver(I) monohydrate, [Ag(hfacNchex)(PPh_3)]·H_2O (7). 1,1,1,5,5,5-Hexafluoro-2,4-pentanedionato(triphenylphosphine)silver(I) (**4**) (4.1 g, 7.0 mmol) was suspended in benzene (150 cm^3) and cyclohexylamine (0.7 g, 7.0 mmol) added. The mixture was gently refluxed in a Dean–Stark apparatus for two hours, to give a yellow-orange mixture, with minimal signs of decomposition. Solvent was removed *in vacuo* to give a sticky oil. The oil was dissolved in diethyl ether, filtered in air and the solvent removed *in vacuo* to give a brown solid. Yield 3.83 g, 81%.

Analysis: found (calculated for $C_{29}H_{29}AgF_6NO_2P$); C, 51.3 (51.5); H, 4.38 (4.32); N, 1.96 (2.07)%. Mp 84 °C. IR (Nujol mull) 1200–1800 cm^{-1}: 1250, 1314, 1325, 1437, 1526, 1599, 1661. IR (hexachlorobutadiene mull) 1200–1800 cm^{-1}: 1252, 1310, 1325, 1373, 1387, 1437, 1451, 1482, 1532, 1559, 1669. ^{1}H NMR ($CDCl_3$) δ: 7.43–7.38 (m, 15H, PPh_3), 5.69 (s, 1H, COCHCO), 2.85–2.65, 2.0–1.8, 1.8–1.65, 1.65–1.55, 1.3–1.15,

1.15–0.95 (C_6H_{11}). ^{13}C NMR ($CDCl_3$) δ: 175.4 (q, 31.9 Hz, CO), 133.8 (d, 16.5 Hz, PPh_3), 131.5 (d, 34.2 Hz, PPh_3), 130.6 (s, PPh_3), 128.9 (d, 9.9, PPh_3), 118.0 (q, 291 Hz, CF_3), 86.0 (s, COCHCO), 36.2 (CH_2), 25.1 (CH_2), 24.8 (CH_2). ^{19}F NMR ($CDCl_3$) δ: -77.2 (CF_3).

Crystallography

A crystal of approximate dimensions $0.4 \times 0.3 \times 0.2$ mm was used for data collection. *Crystal data*: $C_{23}H_{16}O_2F_6PAg$, $M=577.2$ monoclinic, $a=11.175(4)$, $b=17.457(3)$, $c=11.260(3)$ Å, $\beta=101.14(2)^\circ$, $U=2155.0$ Å^3, space group $P2_1/c$, $Z=4$, $D_c=1.78$ g cm^{-3}, μ(Mo-Kα)$=10.7$ cm^{-1}, $F(000)=1144$. Data were measured at 170 K on a CAD4 automatic four-circle diffractometer in the range $2 \geqslant \theta \geqslant 24^\circ$. 3698 Reflections were collected of which 2848 were unique with $I \geqslant 2\sigma(I)$. Data were corrected for Lorentz and polarization effects but not for absorption. The structure was solved by Patterson methods and refined using the SHELX[26,27] suite of programs. In the final least squares cycles all atoms were allowed to vibrate anisotropically. Hydrogen atoms were included at calculated positions except for H(211) [attached to C(21)] which was located in an advanced difference Fourier map and refined at a distance of 0.98 Å from the parent atom. Final residuals after 10 cycles of least squares were $R=0.0407$, $R_w=0.0459$, for a weighting scheme of $w=2.1494/[\sigma^2(F)+0.001252(F)^2]$. Max. final shift/esd was 0.001. The max. and min. residual densities were 0.51 and -0.66 e Å^{-3} respectively. The asymmetric unit is shown in Fig. 2, along with the labelling scheme used and selected metrical data.

Full crystallographic details, excluding structure factors, have been deposited at the Cambridge Crystallographic Data Centre (CCDC). See 'Information for Authors', *J. Mater. Chem.*, Issue 1, available *via* the RSC web page (http://www.rsc.org/authors). Any request to the CCDC for this material should quote the full literature citation and the reference number 1145/166.

Results and discussion

Synthesis and spectroscopy

A series of triphenylphosphine adducts of silver β-diketonates (**1–4**) have been prepared where the ligand substituents have been varied (eqn. (1)). The addition of one molar equivalent of triphenylphosphine to a silver β-diketonate produced, in all but one case, 1 : 1 (Ag : PPh_3) adducts, in good yields (71–86%). The reaction of silver oxide, Hfod and triphenylphosphine, however, resulted in the isolation of a complex **5** with the unexpected formula $[Ag(fod)]_3(PPh_3)_5$, and in lower yield (28%). The compounds **1–5** could be stored at room temperature in the absence of light for extended periods with only moderate decomposition (observed as a darkening of the solid). The observed stability for the complexes at room

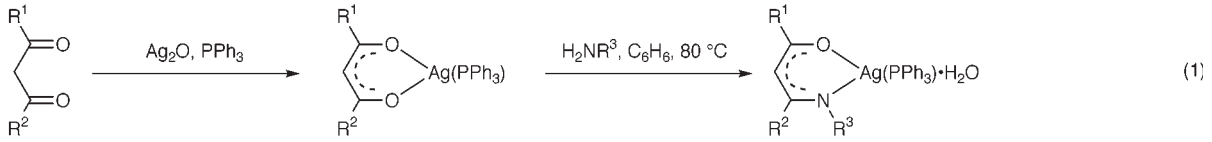

(1)

$R^1 = CH_3$ $R^2 = CH_3$: acac
$R^1 = {}^tBu$ $R^2 = {}^tBu$: dpm
$R^1 = CH_3$ $R^2 = CF_3$: tfac
$R^1 = CF_3$ $R^2 = CF_3$: hfac
$R^1 = {}^tBu$ $R^2 = C_3F_7$: fod

$R^1 = CH_3$ $R^2 = CH_3$ (**1**)
$R^1 = {}^tBu$ $R^2 = {}^tBu$ (**2**)
$R^1 = CH_3$ $R^2 = CF_3$ (**3**)
$R^1 = CF_3$ $R^2 = CF_3$ (**4**)
$R^1 = {}^tBu$ $R^2 = C_3F_7$ [**5**; 3:5 Ag(fod):PPh_3]

$R^1 = CF_3$ $R^2 = CF_3$ $R^3 =$ *n*-hexyl (**6**)
$R^1 = CF_3$ $R^2 = CF_3$ $R^3 =$ cyclohexyl (**7**)

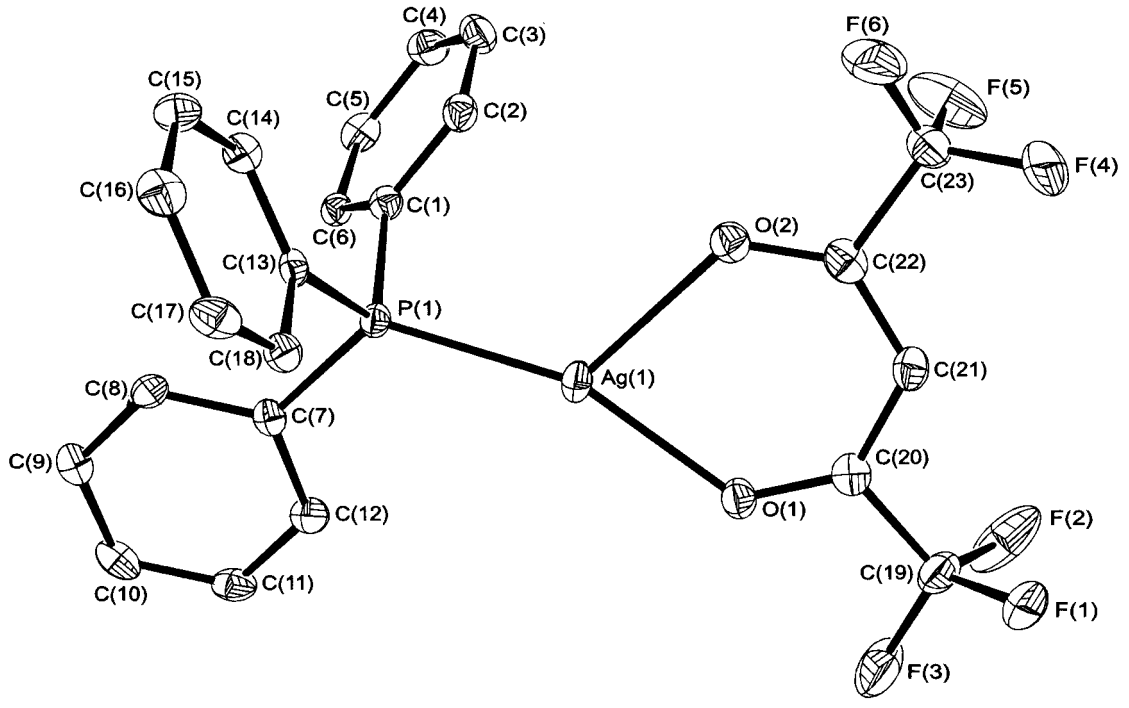

Fig. 2 The structure of **4**. Selected geometric data: Ag(1)–P(1) 2.346(3), Ag(1)–O(1) 2.218(5), Ag(1)–O(2) 2.341(5), O(1)–C(20) 1.253(6), O(2)–C(22) 1.240(7) Å; P(1)–Ag(1)–O(1) 158.7(1), P(1)–Ag(1)–O(2) 119.2(2), O(1)–Ag(1)–O(2) 81.8(2), Ag(1)–O(1)–C(20) 128.9(4), Ag(1)–O(2)–C(22) 125.8(4)°.

temperature is in the order; hfac > tfac ≈ fod > dpm > acac. Initial decomposition points for the non-fluorinated adducts were considerably lower [**1** 150, **2** 140 °C] than for the fluorinated compounds [**3** 200, **4** 250, **5** 210 °C].

Two triphenylphosphine adducts of silver β-ketoiminates have also been synthesised, by the condensation reaction of [Ag(hfac)(PPh_3)] (**4**) with H_2NR (R = *n*-hexyl, cyclohexyl) (eqn. (1)). Complex **4** was chosen for this reaction owing to its higher thermal stability compared to the other β-diketonate adducts. In addition, benzene was used as solvent since the use of the higher boiling toluene met with high rates of decomposition. The 1 : 1 adducts were isolated as hydrates, as evidenced by microanalysis and infra-red spectra, despite the observed removal of water during the reaction over two hours. Preparative yields were high (81–89%). Attempts at the recrystallisation of **6** in air resulted in hydrolysis and reversion to the β-diketonate adduct. Decomposition temperatures for the β-ketoiminato complexes [**6** 100, **7** 115 °C] were lower than for the parent β-diketonate [**4** 250 °C].

^{1}H, ^{13}C and ^{19}F NMR spectra of compounds **1–4** are largely unexceptional, though the integration ratios serve to confirm the adduct stoichiometry as 1 : 1. Carbonyl resonances in the ^{13}C NMR were relatively easily assigned except for the cases of unsymmetrical β-diketonates [**3, 5**] where two different ^{13}C–O resonances were observed, but these could be distinguished by ^2J(CF) couplings to the CF_3 or C_3F_7 groups.

The β-ketoiminate adducts **6** and **7** showed ^{1}H, ^{13}C and ^{19}F NMR resonances shifted from those of complex **4**, the β-diketonate analogue. However, the expected resonances for *C*=NR could not be identified and only one resonance in both the ^{13}C and ^{19}F spectra could be identified for the two non-equivalent CF_3 groups. Such spectroscopic data suggest that the β-ketoiminates may have reverted to the β-diketonate and free amine on standing in solution.

^{31}P resonances of compounds **1–7** were observed as broadened singlets at room temperature, between δ 9 and 26. The absence of ^1J(Ag–^{31}P) coupling indicates a significant dynamic equilibrium due to lability of the ligands.[15,16,28,29] The ^{31}P NMR of **4**, recrystallised several times, showed, however, a sharp doublet of doublets at room temperature indicating that phosphine lability is somewhat dependent on purity, *i.e.* dynamic equilibrium may be reduced if traces of free phosphine are absent. ^1J(^{109}Ag–^{31}P) coupling of 822 Hz in this case was comparable to that found in the ^{109}Ag NMR spectrum at −80 °C (831 Hz) and to reported values of ^1J(^{107}Ag–^{31}P) observed for [Ag(β-diketonate)(PR_3)] (β-diketonate = hfac, fod; R = Me, Et) at low temperature [^1J(^{107}Ag–^{31}P) = 702–760 Hz, ^1J(^{109}Ag–^{31}P)/^1J(^{107}Ag–^{31}P) ≈ 1.15].[16,30]

^{109}Ag resonances observed at low temperature were doublets [with the exception of **5**] and were found in the range δ 513–641 with ^1J coupling of 720–830 Hz. There are no reports of ^{109}Ag NMR chemical shift values in the literature for silver(I) β-diketonates although the observed chemical shifts for these adducts (δ 513–613) are approximately midway between values we have observed for analogous silver carboxylates, [Ag(O_2CR)] (δ *ca.* 170–300) and [Ag(O_2CR)(PPh_3)$_2$] complexes (δ *ca.* 800–930),[31] and are thus diagnostic of monophosphine adducts. The chemical shift for the adducts moves to higher field with increasing fluorination of the β-diketonate. The signal multiplicity (doublets) is also consistent with a single phosphine ligand bound to silver and coupling constants compare well to those found in the literature, *e.g.* [AgX(PR_3)] (R = 2,4,6-trimethoxyphenyl; X = Cl, Br, I) ^1J(^{109}Ag–^{31}P) = 745–821 Hz.[28] The ^{109}Ag NMR spectrum of the β-ketoiminate **7** shows the expected doublet but at lower field (δ 641) than the β-diketonates, the ^1J(^{31}P–^{109}Ag) coupling again being typical for monophosphine adducts (726 Hz).

The spectral data for [Ag_3(fod)$_3$(PPh_3)$_5$] (**5**) is more complex in that three resonances were identified in the ^{109}Ag NMR indicating the presence of three different silver environments in solution. A doublet at δ 564 [^1J(^{31}P–^{109}Ag) = 800 Hz] is very similar to that observed for the other [Ag(β-diketonate)(PPh_3)] complexes, while the remaining resonances are observed as triplets at δ 943 and 823 indicating two phosphine ligands bound to each silver. Coupling constants for these resonances (496 and 523 Hz respectively) concur with this conclusion and compare favourably with reported ^1J(^{107}Ag–^{31}P) for bis-phosphine adducts, *e.g.* [Ag(hfac)(PEt_3)$_2$] (468 Hz).[19] Silver β-diketonate structures have been reported containing two, but not three, distinct silver environments, *e.g.* [Ag(hfac)]$_2$·H_2O.[24] Proposals for potential molecular species consistent with this spectrum are complicated by the fact that in both the ^{1}H and ^{13}C NMR spectra only one type of β-diketonate ligand is observed, although it may be the case that these nuclei are so remote as to remain equivalent. There also remains the possibility that in solution **5** dissociates into a number of smaller oligomers, for instance a dimer (containing inequivalent silver atoms) and a monomer. This structural conundrum awaits crystallographic resolution.

Crystallography

The solid state structure of **4** consists of a silver centre bound by a chelating *O,O′*-hexafluoro-2,4-pentanedionato ligand and a single triphenylphosphine in a distorted trigonal arrangement (Fig. 2). The β-diketonate ligand is unsymmetrically bound resulting in the structure tending towards a linear P–Ag–O1 configuration (P–Ag–O1: 158.7°, P–Ag–O2: 119.2°) with significantly different Ag–O bond lengths [2.218(5), 2.341(3) Å]. This distortion is similar to that found in other silver β-diketonate adducts, although in the case of **4** the difference in P–Ag–O angles is exaggerated: **4**: 39.5°; [Ag(hfac)(PMe_3)]: 3.1, 8.2, 16.2°;[16] [Ag(hfac)(CNMe)]: 24°.[21] Perturbations from the expected trigonal geometry in the two literature examples have been attributed to either packing effects or possible intermolecular H···F interactions (2.235 Å), respectively. In the case of **4**, the nearest H···F interactions are 2.561 Å (intramolecular) and 2.485 Å (intermolecular) which suggests that such interactions are unlikely to be the cause of any distortions. Mean Ag–O bond lengths for **4** (2.28 Å) are comparable with those found in monomeric [Ag(hfac)(PMe_3)] (2.29 Å)[16] and [Ag(hfac)(CNMe)] (2.28 Å)[21] and significantly shorter than Ag–O in silver β-diketonates (typically 2.35–2.64),[14,24,29,32] where Ag is greater than three-coordinate. The Ag–P distance [2.346(3) Å] is slightly longer than that found for the trimethylphosphine adduct, [Ag(hfac)(PMe_3)], (2.32 Å).[16]

The structure of **4** also shows weak intermolecular contacts which result in the formation of dimers (Fig. 3(top)). The two hfac ligands stack in a 'head-to-tail' manner which results in contacts between silver and the methine carbon C(21′)(3.49 Å) and also one fluorine from each of the CF_3 groups [Ag–F(1′) 3.74, Ag–F(4′) 3.39 Å]. Such interactions are long and the weakness of the dimerisation is further evident in the slipped nature of the stack (Fig. 3(bottom)) and the essentially trigonal planar geometry at the metal. In contrast, (fod)Ag(CH_2=$CHSiEt_3$) has a similar dimeric arrangement but one in which the methine carbon sits directly above silver at short range [2.423(7) Å] and generates a distorted tetrahedral geometry about the metal.[22] The Ag···F interactions in **4** do not, however, result in deposition of AgF, nor is there any evidence of fluorine in the deposited silver films. Presumably, dimerisation is destroyed by dissolution in the solutions used in the AACVD experiments.

Decomposition and deposition studies

TGA of **1–7** were carried out under air-purged or helium-purged conditions (Table 2). Thermal degradation of

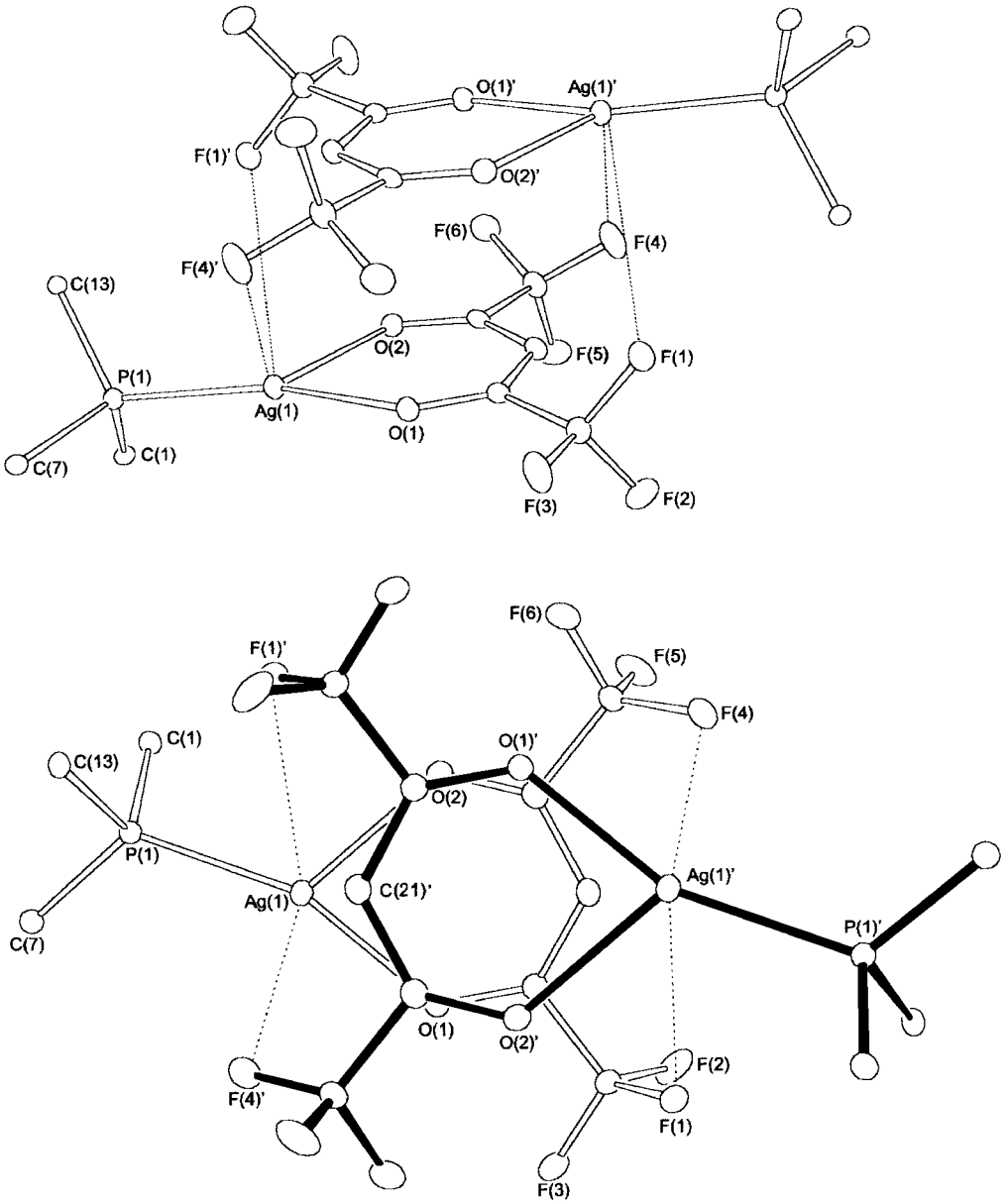

Fig. 3 The dimeric nature of **4** (top) showing the stacking of the hfac ligands and (bottom) highlighting the slipped nature of the stack. Only the α-carbons of the Ph_3P groups are included for clarity. Selected geometric data: Ag–C(21′) 3.49, Ag–F(1′) 3.74, Ag–F(4′) 3.39 Å.

the β-diketonate adducts proceeded in a single step in all cases except **1**, starting between 140 and 250 °C and being complete by 320–350 °C. Maximum rates of decomposition were in the region 270–320 °C. Decomposition of **1** was observed to occur in several stages with maximum rates of decomposition occurring at 190 and 290 °C. As expected, an increase in fluorine content of the β-diketonate had a beneficial effect on the thermal stability.

Thermal degradations of silver β-ketoiminate adducts **6** and **7** were observed to proceed in two overlapping stages. The first step commenced at 100–115 °C, rising to a maximum at 198–206 °C. After this temperature the rate of weight loss

Table 2 Thermal analysis data for silver(I) β-diketonate and β-ketoiminate adducts[a]

		Decomposition temperature/°C			Residue remaining (%)	
Compound		Start[b]	Maxima[c]	End[d]	Calc. % Ag[e]	Found
$Ag(acac)(PPh_3)$	**1**	150	191, 287	330	23.0	24.1
$Ag(dpm)(PPh_3)$	**2**	140	297	320	19.5	18.4
$Ag(tfac)(PPh_3)$	**3**	200	269	330	20.6	20.9
$Ag(hfac)(PPh_3)$	**4**	250	315	350	18.7	17.7
$[Ag(fod)]_3(PPh_3)_5$	**5**	220	310	320	12.8	11.0
$Ag(hfacNhex)(PPh_3)$	**6**	100	198, 314	340	15.9	17.4
$Ag(hfacNchex)(PPh_3)$	**7**	115	206, 304	320	16.0	15.8

[a]TGA experiments were run under an air purged atmosphere except for **7** which was carried out under a He purge. [b]Temperature corresponding to the onset of decomposition. [c]Temperature(s) at which the rate of weight loss is at a maximum. [d]Temperature at which decomposition is complete. [e]Calculated % mass of silver in undecomposed compounds.

declined with increasing temperatures to about 250 °C. This first stage of decomposition in both cases resulted in a weight loss of about 25%, somewhat larger than can be accounted for by the elimination of H_2NR alone (about 15% in both cases). At *ca.* 250 °C the second stage of decomposition rapidly completes the degradation, which is over by 320–340 °C. It should be noted that TGA experiments for **6** and **7** were carried out under air and helium, respectively and this appears to have not drastically influenced their decomposition profiles.

In all seven cases, the mass of residue remaining is consistent with silver metal, though some compounds show evidence of volatility (**2**, **4**, **5**), while other residues (**1**, **4**, **6**) have small amounts of additional material.

Compounds **1–7** were screened as potential precursors for the deposition of silver films using aerosol-assisted chemical vapour deposition methodology (AACVD). The results are collected in Tables 3 and 4. Films were grown under nitrogen using fixed conditions of 310 °C and atmospheric pressure. Precursors were dissolved in THF, the solution nebulised and the resulting mist swept into the reactor deposition chamber using nitrogen carrier gas (Fig. 1). Films were grown on glass substrates. The films were observed to be soft, and although they adhered well to the substrate, they could easily be damaged by scratching or wiping. Films were examined by visual inspection and scanning electron microscopy. Film thickness was estimated using quantitative electron probe microanalysis (EDXS) and contaminants were also identified using this technique; coatings grown from **3** and **6** were further characterised by Auger techniques and high resolution scanning electron microscopy (HRSEM). Where possible, films were characterised with respect to reflectivity and conductivity.

Compounds **1** and **2** (the silver non-fluorinated β-diketonate adducts) were very ineffective at silver film growth under the conditions described. Despite a number of attempts, only faint transparent films could be observed and these were of

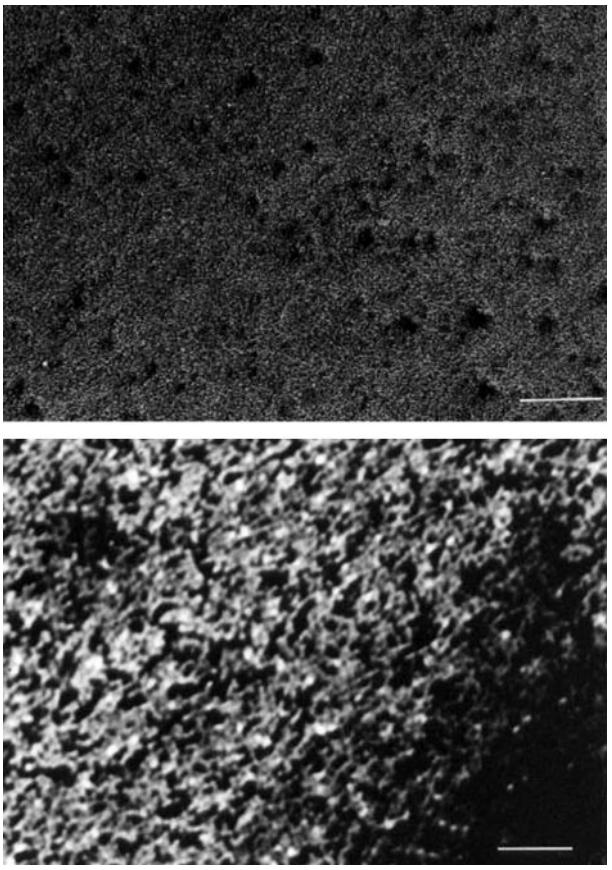

Fig. 4 Scanning electron micrograph at 10 kV of a silver film obtained from the AACVD of $[Ag(fod)]_3(PPh_3)_5$ (**5**), bar = 10 μm (*top*), 1 μm (*bottom*).

Table 3 Properties of silver films grown from silver β-diketonate and silver β-ketoiminate adducts

Compound		Estimated film/ thickness/Å	Deposition time/ min	Estimated deposition rate/ Å min^{-1}	% Reflectance[a]		Sheet resistance/Ω □$^{-1}$[b]
					Coating	Glass	
$Ag(acac)(PPh_3)$	**1**	—	19	—	12.9	10.9	∞
$Ag(dpm)(PPh_3)$	**2**	—	20	—	12.2	10.5	∞
$Ag(tfac)(PPh_3)$	**3**	320[c]	20	>16[c]	62.5	70.3	2.2
$Ag(hfac)(PPh_3)$	**4**	306	29	10.6	0.3	18.0	186
$[Ag(fod)]_3(PPh_3)_5$	**5**	167	22	7.6	19.4	19.8	∞
$Ag(hfacNhex)(PPh_3)$	**6**	295	18	16.4	64.7	85.3	1.1
$Ag(hfacNchex)(PPh_3)$	**7**	248	13	19.1	51.4	30.0	167

[a] $\lambda = 550$ nm corresponding to the peak in the eye response curve. [b] Sheet resistance was measured over a 25 mm square. [c] Owing to the thickness of this film, counts of X-rays from the film were approximately equal to those obtained from the pure Ag bulk sample, the film thickness for this sample may be in excess of this estimate.

Table 4 Appearance of silver films grown from silver β-diketonate and silver β-ketoiminate adducts

Compound		Visual appearance	SEM appearance	Impurities[a,b]	Figure
$Ag(acac)(PPh_3)$	**1**	very faint transparent yellow marks	thin, discontinuous or non-conducting film	—	—
$Ag(dpm)(PPh_3)$	**2**	faint transparent yellow film	thin, discontinuous or non-conducting film	C	—
$Ag(tfac)(PPh_3)$	**3**	heavy deposition, highly reflective in areas, dark grey matt area at downstream side	fairly smooth, regular surface	C	6, 8, 10
$Ag(hfac)(PPh_3)$	**4**	thick grey matt film, not particularly reflective	even surface comprised of a thick mat of long, thin crystals	C, P(trace)	5
$[Ag(fod)]_3(PPh_3)_5$	**5**	reflective silver film	uneven film with high concentration of surface protrusions	C	4
$Ag(hfacNhex)(PPh_3)$	**6**	reflective film, slightly matt white in areas of heaviest deposition	fairly smooth, even surface	C	7, 9
$Ag(hfacNchex)(PPh_3)$	**7**	reflective silver film on entire substrate, whitish matt in areas of heaviest deposition	fairly smooth although undulating	C	—

[a] Measured by EDXS; the presence of oxygen in the films was masked by oxygen detected in the glass. [b] Trace quantities were at the limits of detection of the instrumentation.

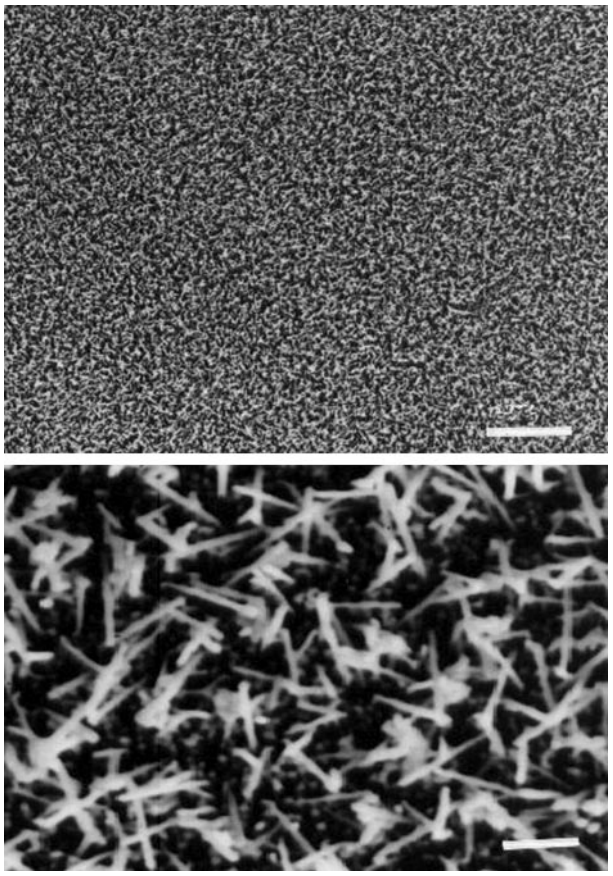

Fig. 5 Scanning electron micrograph at 10 kV of a silver film obtained from the AACVD of Ag(hfac)(PPh_3) (**4**), bar = 10 μm (*top*), 1 μm (*bottom*).

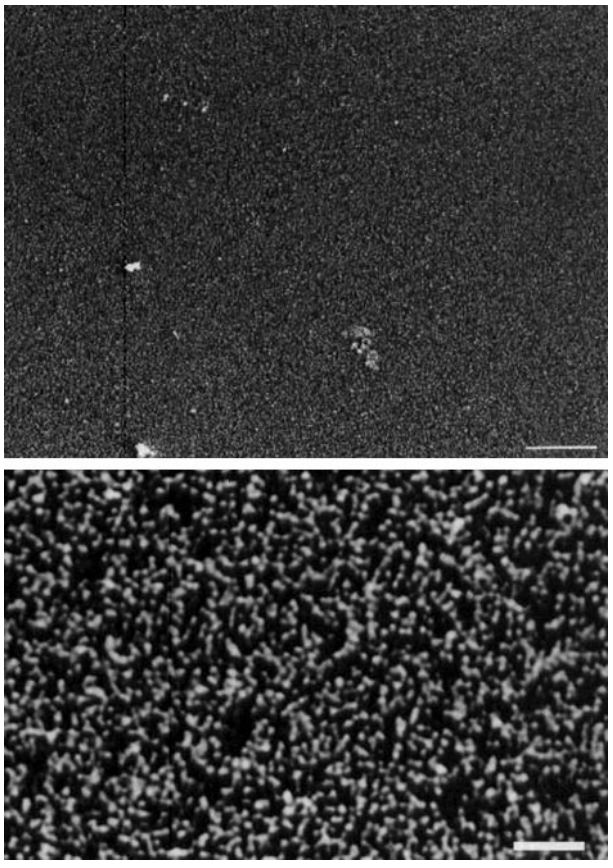

Fig. 6 Scanning electron micrograph at 10 kV of a silver film obtained from the AACVD of Ag(tfac)(PPh_3) (**3**), bar = 10 μm (*top*), 1 μm (*bottom*).

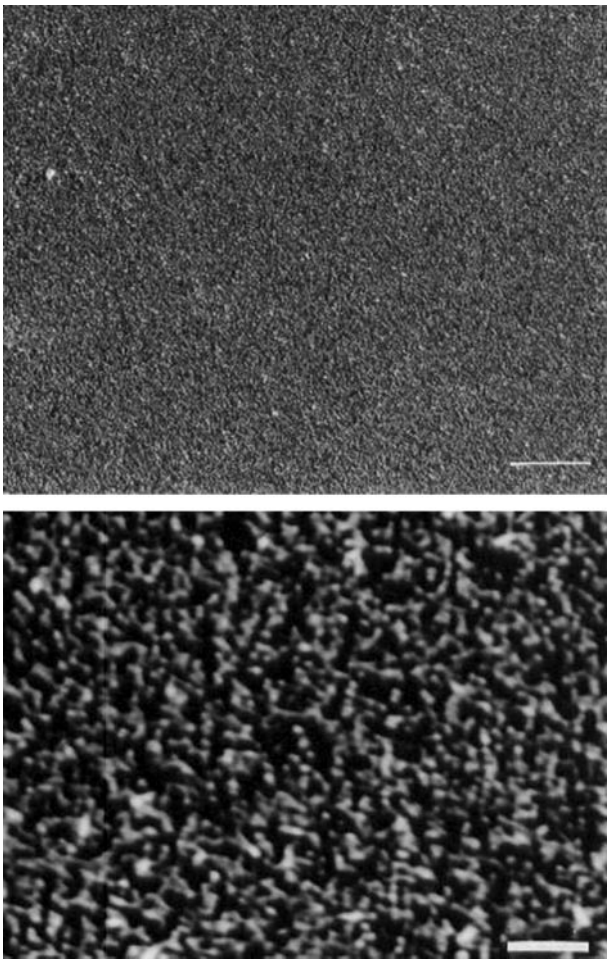

Fig. 7 Scanning electron micrograph at 10 kV of a silver film obtained from the AACVD of Ag(hfacNhex)(PPh_3) (**6**), bar = 10 μm (*top*), 1 μm (*bottom*).

insufficient quality to characterise fully. The remainder of compounds tested (**3–7**) (silver fluorinated β-diketonate and silver β-ketoiminate adducts) were all capable of growing silver-containing films. In terms of growth rates (Table 3), **5** was the least effective of the fluorinated precursors (7.6 Å min^{-1}), while of the silver β-diketonates **3** grew at the fastest rate (> 16 Å min^{-1}). Growth rates of the silver β-ketoiminate adducts **6** and **7** exceeded those measured for their parent silver β-diketonate adduct **4** and the coatings appeared more reflective. The fastest growth rates for any of the adducts studied was for **7**, which was estimated to exceed 19 Å min^{-1}.

Deposition rates appear to have no obvious relationship with decomposition points and all of these precursors would have been expected to show high rates of decomposition at the substrate temperature used (310 °C). The β-ketoiminate adducts were found to start decomposition at much lower temperatures than fluorinated β-diketonates (Table 2) and yet displayed film growth rates of the same order of magnitude.

Films grown from compounds **3–7** were examined at 10000× magnification by SEM (Table 4). The surface of the film grown from **5** was found to be uneven with a high concentration of protrusions from the bulk surface (Fig. 4). The surface of the film from **4** was observed to resemble a thick mat of long, thin crystals (Fig. 5) while films grown from **3** (Fig. 6), **6** (Fig. 7), and **7** (not shown) appeared as fairly uniform, smooth films at the magnification used. HRSEM at higher magnification (50000×) on coatings grown from **3** and **6** revealed that these two films are made up from several layers of loosely packed spheres of silver (Fig. 8 and 9), the size of the spheres being approximately 500–1000 Å.

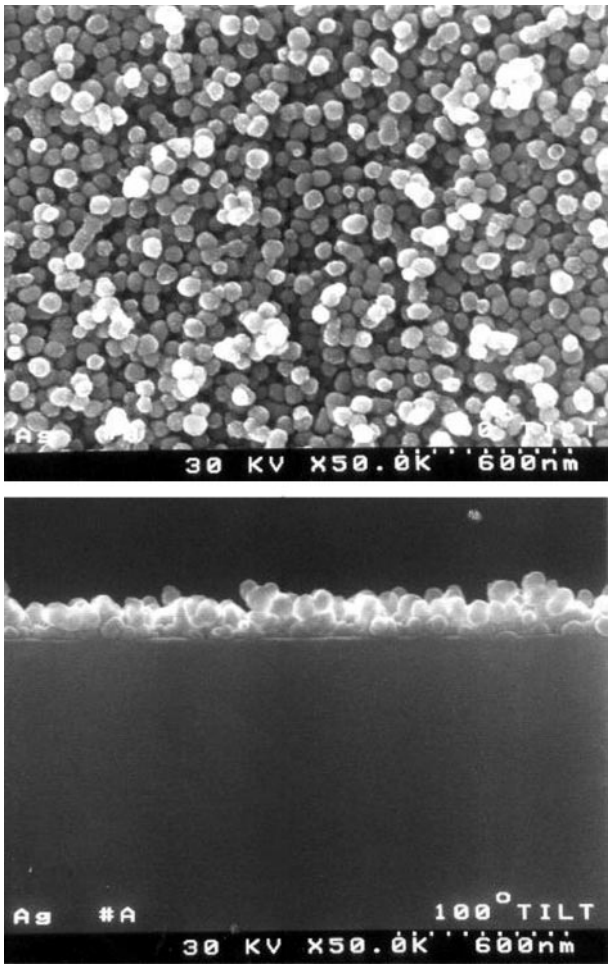

Fig. 8 High resolution scanning electron micrographs at 30 kV of a silver film obtained from the AACVD of Ag(tfac)(PPh_3) (**3**).

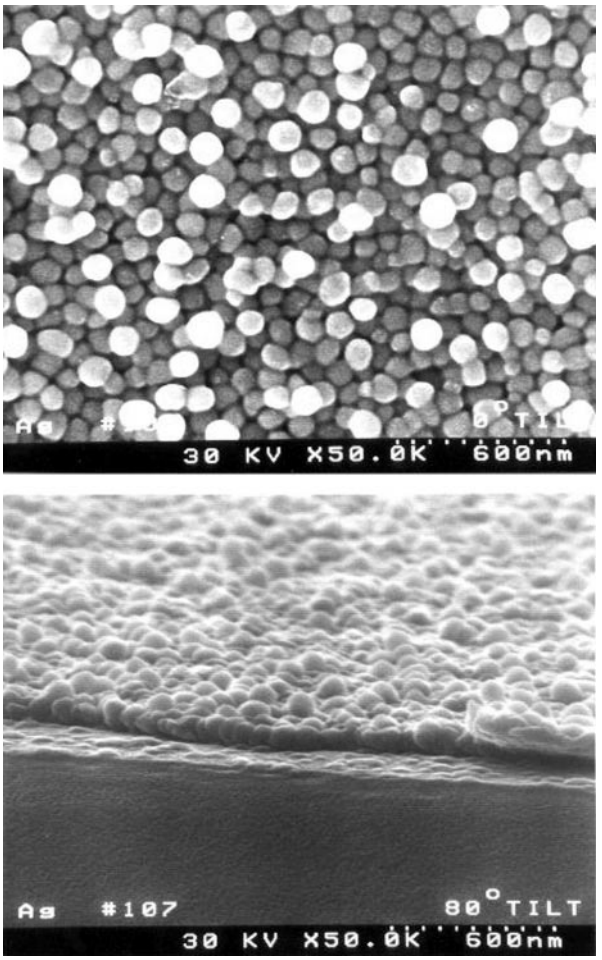

Fig. 9 High resolution scanning electron micrographs at 30 kV of a silver film obtained from the AACVD of Ag(hfacNhex)(PPh_3) (**6**).

Carbon (5–10%) was the only consistent contaminant in all the films, as detected by EDXS. This impurity appears independent of both precursor and film thickness, and is of comparable levels in each of the films grown.

The presence of oxygen contaminants in the films was difficult to assess due to the masking effect of the glass substrate. However, in the case of very thick films, the X-rays characteristic of oxygen were considerably reduced and the intensity ratio of silicon to oxygen peaks appeared to be fairly constant. This suggests that oxygen contamination is at worst no higher than carbon contamination. Trace phosphorus contamination was detected only in the film grown from **4** and no fluorine was detected in any of the films. Subsequent Auger depth profiling analysis of the films grown from **3** (Fig. 10) and **6** has confirmed that these films are predominantly silver (91.3–91.5 atom%) with carbon (6.4–7.5 atom%) and trace oxygen (1.2–2.0 atom%). Fluorine and phosphorus contaminants were not detected and this concurs with the EDXS studies. Such film analysis results compare favourably with reports on films deposited by low-pressure thermal CVD of [Ag(β-diketonate)L] (β-diketonate = hfac, fod; L = PMe_3, PEt_3) where, in the absence of hydrogen, contamination was of the order of 5–35% carbon, 5% oxygen with trace fluorine and phosphorus.[16]

Reflectance studies (Table 3) on films grown from precursors **1–7** included measurements from both the coated surface and from the film–glass interface (*i.e.* through the glass). Metallic films on glass generally exhibit lower reflectance from the coating surface as compared to the coating–glass interface, this being primarily a function of surface roughness and its ability to scatter light. Films grown from precursors **1** and **2** gave poor reflectance results. Films deposited from **5** appeared considerably more reflective by visual inspection although measured reflectivity at 550 nm was less than 20%. The sheet resistances (Table 2) of films grown from **1**, **2** and **5** were not quantifiable.

Films deposited with precursors **3**, **6** and **7** gave highly reflective films with reflectance from the coating surface of 50–65% and reflectivity from the glass–coating interface of up to 85%. Coatings grown using **4** as the precursor gave thick matt films which had poor reflectivity from both surfaces, which was surprising as similar precursors have been widely studied in the literature.[8,22,24] All films grown from **3**, **4**, **6**, **7** (estimated thickness 250–320 Å; Table 3) had a measurable sheet resistance, with sheet resistances of 1.1 $\Omega\,\square^{-1}$ (**6**) and 2.2 $\Omega\,\square^{-1}$ (**3**) being the lowest observed during the course of these studies. From the data displayed in Table 3 there appears to be an approximate correlation between reflectance and sheet resistance but not between reflectance and deposition rate, which may suggest that reflectance is affected largely by impurities rather than by surface morphology.

4. Conclusions

This paper reports the first broad survey of the potential utility of silver(I) compounds as precursors for the formation of silver films by AACVD. All the compounds investigated involve chelating β-diketonates or β-ketoiminate ligands and incorporate the cheap, widely available PPh_3 ligand, hitherto ignored in silver deposition because of the low volatility of its adducts.

The results obtained suggest that the β-ketoiminate complexes show greater potential, affording lower initial

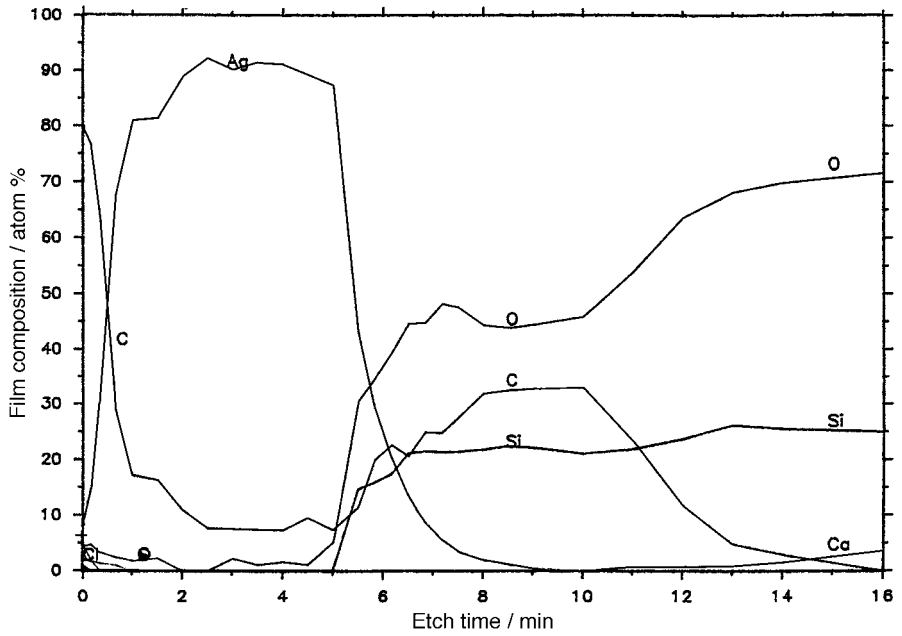

Fig. 10 Auger depth profile analysis of a silver film obtained from the AACVD of Ag(tfac)PPh_3 (**3**). Elemental analysis: Ag 91.3, C 7.5, O 1.2%.

decomposition temperatures and somewhat higher deposition rates. The films produced are smoother, of good thickness with relatively low impurity levels combined with acceptable reflectivities. The two-stage synthesis required to generate such precursors along with their relative hydrolytic instability with respect to the analogous β-diketonates remain, however, disadvantages.

We thank the EPSRC and Pilkington plc for support (R.M.H.) in the form of a CASE award.

References

1 M. L. Green, M. E. Gross, L. E. Papa, K. J. Schnoes and D. Brasen, *J. Electrochem. Soc.*, 1985, **132**, 2677.
2 S. Motojima, S. Kuri and T. Hattori, *J. Less-Common Met.*, 1986, **124**, 193.
3 J. P. Lu, P. W. Chu, R. Raj and H. Gysling, *Thin Solid Films*, 1992, **208**, 172.
4 C. Y. Xu and T. H. Braum, *Chem. Mater.*, 1998, **10**, 2329.
5 N. H. Dryden, R. Kumar, E. C. Ou, M. Rashidi, S. Roy, P. R. Norton, R. J. Puddephatt and J. D. Scott, *Chem. Mater.*, 1991, **3**, 677.
6 H.-K. Shin, K. M. Chi, J. Farkas, M. J. Hampden-Smith, T. T. Kodas and E. N. Duesler, *Inorg. Chem.*, 1992, **31**, 424.
7 M. Hoshino, *Gold Bull.*, 1994, **27**, 2.
8 R. J. H. Voorhoeve and J. W. Merewether, *J. Electrochem. Soc.*, 1972, **119**, 364.
9 M. J. Shapiro, W. J. Lackey, J. A. Hanigofsky, D. N. Hill, W. B. Carter and E. K. Barefield, *J. Alloys Compd.*, 1992, **187**, 331.
10 Anonymous, *Res. Discl.*, 1986, **263**, 146.
11 C. Oehr and H. Suhr, *Appl. Phys. A*, 1989, **49**, 691.
12 P. M. Jeffries, S. R. Wilson and G. S. Girolami, *J. Organomet. Chem.*, 1993, **449**, 203.
13 C. D. M. Beverwijk, G. J. M. van der Kerk, A. J. Leusink and J. Noltes, *J. Organomet. Chem. Rev.*, 1970, **5**, 215.
14 W. Lin, T. H. Warren, R. G. Nuzzo and G. S. Girolami, *J. Am. Chem. Soc.*, 1993, **115**, 11644.
15 N. H. Dryden, J. J. Vittal and R. J. Puddephatt, *Chem. Mater.*, 1993, **5**, 765.
16 Z. Yuan, N. H. Dryden, J. J. Vittal and R. J. Puddephatt, *Chem. Mater.*, 1995, **7**, 1696.
17 S. Serghini-Monim, Z. Yuan, K. Griffiths, P. R. Norton and R. J. Puddephatt, *J. Am. Chem. Soc.*, 1995, **117**, 4030.
18 C. Xu, M. J. Hampden-Smith and T. T. Kodas, *Adv. Mater.*, 1994, **6**, 746.
19 C. Xu, M. J. Hampden-Smith and T. T. Kodas, *Chem. Mater.*, 1995, **7**, 1539.
20 T. H. Baum, C. E. Larson and S. K. Reynolds, *US Patent*, 5 096 737, 1992.
21 Z. Yuan, N. H. Dryden, X. Li, J. J. Vittal and R. J. Puddephatt, *J. Mater. Chem.*, 1995, **5**, 303.
22 K.-M. Chi, K.-H. Chen, S.-M. Peng and G.-H. Lee, *Organometallics*, 1996, **15**, 2575.
23 C. Xu, M. J. Hampden-Smith, T. T. Kodas, E. N. Duesler, A. L. Rheingold and G. Yap, *Inorg. Chem.*, 1995, **34**, 4767.
24 C. Y. Xu, T. S. Corbitt, M. J. Hampden-Smith, T. T. Kodas and E. N. Duesler, *J. Chem. Soc., Dalton Trans.*, 1994, 2841.
25 D. Gibson, B. F. G. Johnson and J. Lewis, *J. Chem. Soc. (A)*, 1970, 367.
26 G. M. Sheldrick, in SHELX76, A program for crystal structure determination, University of Cambridge, 1976.
27 G. M. Sheldrick, in SHELX86, A program for crystal structure determination, University of Gottingen, 1986.
28 L. J. Baker, G. A. Bowmaker, D. Camp, Effendy, P. C. Healy, H. Schmidbaur, O. Steigelmann and A. H. White, *Inorg. Chem.*, 1992, **31**, 3656.
29 Z. Yuan, N. H. Dryden, J. J. Vittal and R. J. Puddephatt, *Can. J. Chem.*, 1994, **72**, 1605.
30 E. L. Muetterties and W. Alegranti, *J. Am. Chem. Soc.*, 1972, **94**, 6386.
31 R. Harker, PhD thesis, University of Bath, 1996.
32 A. Bailey, T. S. Corbitt, M. J. Hampden-Smith, E. N. Duesler and T. T. Kodas, *Polyhedron*, 1993, **12**, 1785.

Paper 9/01937E